Optimization of Skin Impedance Sensor Design with Finite Element Simulations

F. Dewarrat[1], L. Falco[1], A. Caduff [*,1] and M. Talary[1]
[1]Solianis Monitoring AG, Zürich
*Corresponding author: Andreas Caduff, Leutschenbachstrasse 46, 8050 Zürich, andreas.caduff@solianis.com

Abstract: Impedance spectroscopy is a measurement technique that has been investigated in a wide variety of medical applications. An example is the measurement of the dielectric properties of the skin and underlying tissue using sensors placed in contact with human skin with capacitive fringing field electrodes. Electrodes with different characteristic geometries measure biophysical properties at separate penetration depths in the tissue and have therefore different sensitivities to e.g. physiological processes in the tissue. When the measured depth is in the dermis layer, the time series of the measured impedance at specific frequencies can be related to the effect of glucose changes. The aim of this work is to use finite element methods (FEM) for optimizing the sensor design to maximise its sensitivity to the dielectric changes of the dermis layer. This is achieved by evaluating FEM simulations for different electrode widths and distances to ground and searching for the geometries at which the information coming from the dermis layer reach a maximum. Experimental data supports the conclusions drawn from the simulation output.

Keywords: Impedance, skin, penetration depth, glucose monitoring.

1. Introduction

Currently, there is an increasing number of people developing diabetes [1], a disease concerned with the inability of the body to achieve sufficient glucose regulation. The patients should therefore regulate the glucose levels themselves, first by measuring the glucose level and then by moving it to normo-glycemic levels, to avoid the long term illnesses associated with this disease [2]. This self control is made more efficient when the glucose measurements are numerous; therefore there is a need for continuous and preferably non invasive monitoring methods.

Dielectric characterisation of skin and underlying tissue has shown great potential as a non invasive glucose monitoring technique. The underlying measurement principle is related to the change in the dielectric properties of the skin and underlying tissue (particularly of the highly micro-vascularised dermis layer) with glucose level changes. A sensor composed of capacitive fringing field electrodes of different sizes is placed in direct contact to the skin surface which measures the dielectric properties of the underlying tissue. Such a sensor has initially been validated in experimental-clinical trials where it showed its ability to track perturbing factors such as sweat or perfusion changes. Subsequently it has been tested in experimental clinical trials where it was shown that the temporal profile of the measured impedance (or admittance) can be related with the glucose profile [3].

2. Methods

The electrical properties of the sensor skin can be modelled in a simplified approach as being composed of several successive parallel homogeneous layers, as shown in **Figure 1**. Since some layers are very thin, producing a fine meshing for FEM analysis, it is necessary to use the symmetry of the model system to reduce the size of the model complexity. Therefore a 2D cross section of the sensor is a preferred simplification of a full 3D simulation [4].

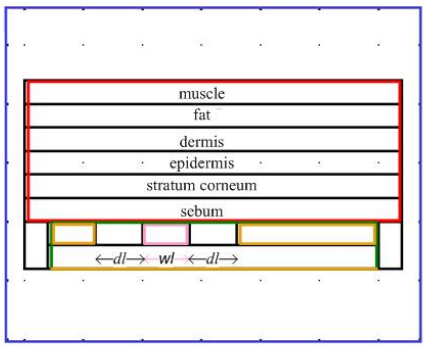

Figure 1. 2D cross section (not to scale) of the impedance sensor (green) with ground electrode

(gold), driven electrode (pink) in contact with skin (orange). The distance *wl* is referred as the electrode width, *dl* as the gap width.

The simulation system is defined by the sensor dimensions, the thickness of the different layers and each domain's dielectric parameters. Since the wavelength of the electric field in the different layers is shorter than the geometric sizes of the electrodes (see below), the quasi static simplification can be used (i.e. Comsol AC/DC Module, 2D Small In Plane Currents application mode).

The equation to be solved is the combination of the Laplace equation and the conservation of charge, with a harmonic applied voltage, i.e.

$$\nabla \cdot \left(\left(\sigma + i\omega\varepsilon_0\varepsilon_r \right) \nabla V \right) = 0 \qquad (1)$$

A harmonic voltage of 1V is applied to the driven electrode, the other electrode is grounded. The backside of the sensor substrate is also grounded and the other simulation boundaries are set to insulating, i.e. there is no current flowing through these external boundaries as expected for the human body. For these simulations the frequency of the applied voltage is set to a constant value of 15 MHz. Simulations on a broader frequency spectrum will be evaluated in future work. The layer thickness and dielectric properties used for the simulations are given in the following table.

Table 1: Layer thickness and dielectric parameters used in the simulation (combination of literature sources [5, 6] or estimation case not explicitly found)

Domain	Thickness [mm]	ε'	σ [S/m]
Sensor substrate	1.5	4.4	0
Sebum	0.01	75	0.001
Stratum Corneum	0.015	10	0.001
Epidermis	0.1	15	0.025
Dermis	1	110	0.2
Fat	1.2	15	0.06
Muscle	20	80	0.7

The wave length λ and the exponential attenuation of the field δ are given by

$$\lambda = 1/\mathrm{Re}(k) = c/(2\pi\nu\,\mathrm{Re}\sqrt{\varepsilon}) \qquad (2)$$

and

$$\delta = 1/\mathrm{Im}(k) = c/(2\pi\nu\,\mathrm{Im}\sqrt{\varepsilon}) \qquad (3)$$

[7]

where *k* is the wave number, *c* is the speed of light, ν the frequency and ε the complex permittivity $\varepsilon = \varepsilon' - i\varepsilon'' = \varepsilon' - i(\sigma/\omega\varepsilon_0)$. The calculation of the smallest values is done with the largest permittivity (110) and conductivity (0.7), which gives $\lambda_{\min} \cong 15\,\mathrm{cm}$ and $\delta_{\min} \cong 17\,\mathrm{cm}$. Since they are significantly larger than the geometric sizes, it allows to neglect the wave character of the electric fields and to use quasi static conditions in the simulations.

The admittance *Y* measured by the electrode (the inverse of the impedance) can be written in the complex form as

$$Y = G + i\omega C, \qquad (4)$$

where *G* is the conductance, ω the angular frequency and *C* the capacitance. The model is valid when the measured material can be described as a conductance and a capacitance in parallel, with no induction term.

The capacitance and the conductance are proportional respectively to the conserved and to the dissipated part of the electric energy placed in the system. Therefore an integration of the energy (conserved and dissipated) over the different domains of the simulation allows the calculation of their relative contribution to the total capacitance and conductance. This is achieved by integrating the time averaged (over a period) electric energy

$$\int_{V_{L_i}} \varepsilon_{L_i} {E_0}^2 dV \qquad (5)$$

And the resistive heating

$$\int_{V_{L_i}} \sigma_{L_i} {E_0}^2 dV \qquad (6)$$

Where V_{Li} is the i[th] layer volume, E_0 the amplitude of the electric field, ε_{Li} the permittivity of the i[th] layer and σ_{Li} its conductivity.

The relative electric energy per layer is obtained by dividing the electric energy in the layer by the electric energy of the whole system.

3. Simulation results

The simulations have been completed for electrode dimension vectors between 0.1 and 6 mm. Two nested loops are run along this vector for the electrode width and for the gap width between the electrode and the ground [8].

The following figures show that the search for a maximum of the electric energy or the resistive heating as a function of the electrode size can help in the electrode design optimization procedure. Examples are shown successively for a fixed electrode width and for a fixed gap width. The quantities shown are the relative electric energy and the relative resistive heating for each layer respectively.

a)

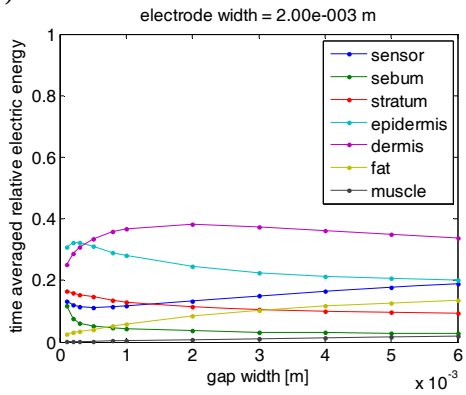

b)

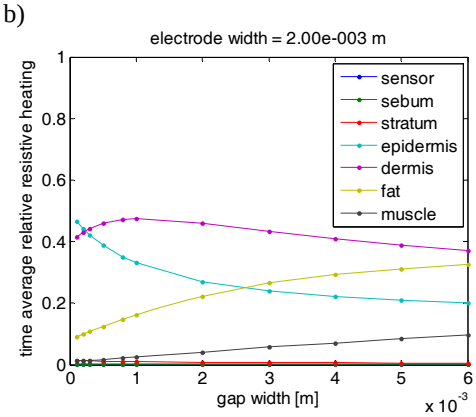

It can be seen from these graphs that for a fixed electrode width, the relative electric energy of the upper skin layers (sebum and stratum corneum) is decreasing for increasing electrode gap widths. The relative electrical energy of the next layer, the epidermis, reaches a maximum for an electrode gap width of around 0.5 mm, and then decreases. A similar effect occurs for the next layer, the dermis, with a maximum at a larger gap width of about 2 mm.

c)

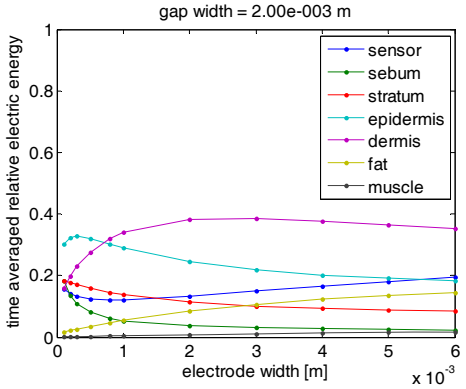

d)

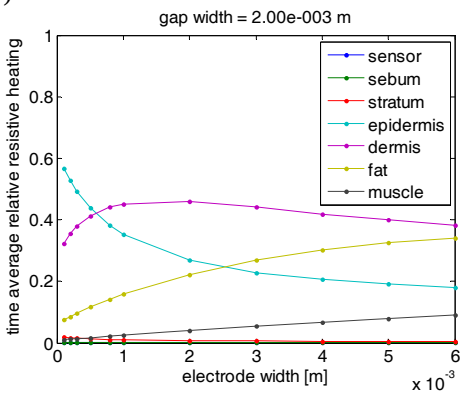

Figure 2. Simulation output versus gap width for a fixed electrode width (a and b) and versus electrode width for a fixed gap width (c and d). The output is the relative electric energy (a and c) and the relative resistive heating (b and d) as defined in eq. 5 and 6. The legend shows over which domain the energy is integrated.

For the deepest skin layers, the fat and muscle, the relative electric energy is continuously increasing with the gap width and does not reach a maximum within the simulation range. The phenomenon is the same when the resistive heating is considered instead of the electric

energy. The conclusion is that the maximum of the contribution of a certain skin layer occurs at a larger electrode gap width for deeper layers. This validates the statement of the increased penetration depth of electric field with larger gap width.

If the gap width is fixed and the electrode width is changed, then the same phenomenon as described above appears, such that the maximum of the resistive heating occurs at larger electrode widths for deeper skin layers.

The maximum of relative electric energy in the dermis layer is obtained at (dl = 2 mm, wl = 3 mm) and the one of resistive heating in is obtained at (dl = 1 mm, wl = 2 mm).

Note that if the quantity to maximize is the energy integrated in the muscle layers, then the search for the optimal electrode sizes yields the largest electrode size given for the simulation, as expected.

4. Experimental results

A comparison of the simulations described above and *in vitro* measurements on 2 layered systems with an impedance sensor was carried out to validate the approximation and to estimate the sensitivity to the different parameters, especially the difference in depth penetration [7].

The *in vivo* experiments shown here were run with a sensor containing three electrodes with different characteristic sizes. The measurement protocol comprised the following steps. After the sensor placement on the subject's upper arm, the glucose concentration in the subject was regulated with oral glucose and intra venous (IV) insulin administration in order to obtain two successive peaks with significant glucose level changes. Total duration of the experiments was around eight hours. During this time patients remained in the same position (comfortable sitting).

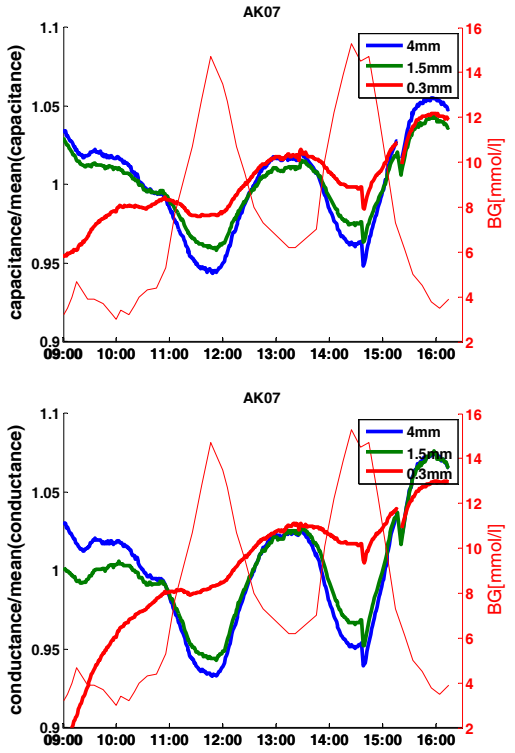

Figure 3. Normalised quantities (capacitance and conductance) measured versus time in hours with electrode of different width and distance to the ground (in legend). The left axis shows the measured reference blood glucose profile.

The Figure 3 shows the measured capacitance and conductance divided by their mean values in order to visually compare them easily on the same graph. It can be seen that the signal measured with the electrode of 0.3 mm width is hardly influenced by the glucose changes but rather follows a daily trend increase. On the contrary, the electrodes of 1.5 and 4 mm show a stronger sensitivity to the glucose changes, since the portion of the measurements coming from the dermis layer is larger for these electrodes.

5. Conclusions

Finite element simulation methods have been used to optimise the geometry of an impedance sensor for a multilayered skin model. An application for such a sensor is in non-invasive continuous glucose monitoring. Continued

efforts are being made to show that such measurement methods can be used in daily life conditions.

8. References

1. S. Wild, G. Roglic, A. Green, R. Sicree, and H. King, Global prevalence of diabetes: estimates for the year 2000 and projections for 2030, *Diabetes Care*, **27** (5), 1047-1053 (2004)
2. American Diabetes Association, Clinical practice recommendations, *Diabetes Care* **22**, 77-78 (1999)
3. M. S. Talary, F. Dewarrat, D. Huber, A. Caduff, In vivo life sign application of dielectric spectroscopy and non-invasive glucose monitorig, *Journal of Non-Crystalline Solids*, **353**, 4515-4517 (2007)
4. M. S. Talary, F. Dewarrat, A. Caduff, A. Puzenko, Y. Ryabov, Y. Feldman, An RCL Sensor for Measuring Dielectrically Lossy Materials in the MHz Frequency Range, *IEEE Transactions on Dielectrics and Electrical Insulation*, **13 (2)**, 247-256 (2006)
5. S. Gabriel, R.W. Lau, C. Gabriel, The dielectric properties of biological tissues: II. Measurements in the frequency range 10 Hz to 20 GHz, *Phys. Med. Biol*., **41**, 2251-2269 (1996)
6. O. G. Martinsen, S. Grimnes, H. P. Schwan, Interface phenomena and dielectric properties of biological tissue, Encyclopedia of Surface and Colloid Science, ed. A. T. Hubbard, 2643-2652 (2002)
7. F. Dewarrat, L. Falco, A. Caduff, M. S. Talary, Y. Feldman, A. Puzenko, Measurement and Simulation of Conductive Dielectric Two-layer Materials with a Multiple Electrodes Sensor, to be published in IEEE Transactions on Dielectrics and Electrical Insulation
8. S. Huclova, J. Fröhlich, unpublished results

9. Acknowledgements

Thanks to D. Lange, S. Hegnauer and D. Huber for valuable discussions.